CASSCF-based explicit ligand field models clarify the ground state electronic structures of transition metal phthalocyanines (MPc; M = Mn, Fe, Co, Ni, Cu, Zn)

Andrew J. Wallace, Bryce E. Williamson, and Deborah L. Crittenden

Abstract: Multireference electronic structure methods are used to assign ground state electronic configurations for a series of metallophthalocyanines. Ligand orbital occupancies remain constant across the period, and are consistent with a formal 2- charge on the ligand. The d electron configurations of some metallophthalocyanines are straightforward and can be unambiguously assigned; $(d_{xy})^2(d_{xz},d_{yz})^{2,2}(d_{z^2})^2(d_{x^2-y^2})^n$, with $n = 2, 1, 0$, respectively, for ZnPc, CuPc and NiPc. Controversies over ground state electronic structure assignments for other metallophthalocyanines arise due to multiple complicating factors; accidental near-degeneracies, environmental effects and different ligand field models used in interpreting experimental spectra. We demonstrate that explicit ligand field models provide more reliable and consistent interpretations of experimental data than implicit, parameterized alternatives. On this basis, we assign gas-phase electronic ground states for MnPc: $(d_{xy})^2(d_{xz},d_{yz})^{1,1}(d_{z^2})^1$, and CoPc: $(d_{xy})^2(d_{xz},d_{yz})^{2,2}(d_{z^2})^1$, and show that the ground state of FePc cannot be resolved to a single state, with two near-degenerate states that are likely spin-orbit coupled: $(d_{xy})^2(d_{xz},d_{yz})^{1,1}(d_{z^2})^2$ and $(d_{xy})^2(d_{xz},d_{yz})^{2,1}(d_{z^2})^1$. Remaining differences between computational predictions and experimental observations are small and may be ascribed primarily to environmental effects, but are also partly due to incomplete modelling of electron correlation.

Keywords: ligand field theory, CASSCF, MRMP2, phthalocyanine, multireference

1. Introduction

As members of the porphinoid family of molecules, phthalocyanines (Figure 1) are of significant practical and theoretical interest.[1] In particular, transition-metal phthalocyanines are widely used as dyes in the textile industry, accounting for around 25% of all organic pigment production worldwide.[2] They are also important in medical applications, filling niche roles as photo-sensitizing agents in anti-cancer photodynamic therapy,[3, 4, 5, 6, 7] and as contrast agents for magnetic resonance imaging.[8]

Over the past 5-10 years, transition-metal phthalocyanines have become the focus of intense and resurgent interest, due to their potential applications in molecular electronics; as key components of light-emitting diodes and organic photovoltaic materials. Despite this, fundamental questions remain about the electronic structure of transition-metal phthalocyanines, with conflicting evidence in the literature supporting different assignments for excited states beyond the first [9, 10], and even disagreement on the nature of the manganese[11, 12, 13] and iron[14, 15, 16, 11, 17, 18, 19, 20] phthalocyanine ground states.

In this paper, we address the latter problem using multireference *ab initio* methods to model the gas-phase ground state electronic structure of transition-metal phthalocyanines, and interpret these results within a ligand field theory framework.[21] It is important to note that explicit *ab initio*-derived ligand field models may produce results that are quite different to those obtained from the more familiar implicit, or parameterized, ligand field models[22] that are commonly used to interpret experimental data.

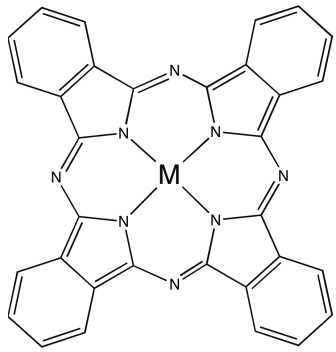

Fig. 1. Metallophthalocyanine chemical structure

Multireference methods also differ substantially from more commonly used single reference approaches such as Hartree-Fock theory and density functional theory, particularly in their ability to appropriately describe degenerate and open-shell states without breaking spatial and/or spin symmetry. They also provide a more balanced treatment of electron correlation across different electronic states, with ground and excited state or-

Andrew J. Wallace, Bryce E. Williamson, and Deborah L. Crittenden.[1]
Department of Chemistry, University of Canterbury,
Private Bag 4800, Christchurch 8140, New Zealand

[1] Corresponding author (e-mail: deborah.crittenden@canterbury.ac.nz).

bitals optimized concurrently, and dynamic correlation corrections applied equally across all states. Hence, multireference models are expected to provide substantially more accurate and robust energies for ground and near-to-ground electronic states than their single reference counterparts.

Existing literature methods and results will be reviewed in detail in the light of the present work. Where appropriate, the influence of environmental effects will also be considered to rationalize differences between gas-phase computational predictions and condensed-phase experimental observations.

2. Methods

To determine ground state orbital energy levels and occupancies for the metallophthalocyanines MnPc, FePc, CoPc and NiPc, complete active space self-consistent field (CASSCF) calculations[23] were carried out using the GAMESS quantum chemistry program package.[24] Active spaces were initially chosen to include five metal-centred orbitals of predominantly ($> 90\%$) d atomic orbital character (d_{xy}, d_{xz}, d_{yz}, $d_{x^2-y^2}$, d_{z^2}). All states accessible by redistributing electrons amongst all occupied d orbitals were equally weighted. For example, for FePc, the following states were averaged over during CASSCF orbital optimization:

$$\begin{aligned}
^3A_{2g}: &\quad (d_{xy})^2(d_{xz},d_{yz})^{1,1}(d_{z^2})^2(d_{x^2-y^2})^0\\
^3E_g: &\quad (d_{xy})^2(d_{xz},d_{yz})^{2,1}(d_{z^2})^1(d_{x^2-y^2})^0\\
&\quad (d_{xy})^2(d_{xz},d_{yz})^{1,2}(d_{z^2})^1(d_{x^2-y^2})^0\\
^3B_{2g}: &\quad (d_{xy})^1(d_{xz},d_{yz})^{2,2}(d_{z^2})^1(d_{x^2-y^2})^0\\
^3E_g: &\quad (d_{xy})^1(d_{xz},d_{yz})^{2,1}(d_{z^2})^2(d_{x^2-y^2})^0\\
&\quad (d_{xy})^1(d_{xz},d_{yz})^{1,2}(d_{z^2})^2(d_{x^2-y^2})^0
\end{aligned}$$

Moving beyond the mean-field approximation, energies for the ground and near-to-ground electronic states were refined using multi-reference second-order Moller-Plesset perturbation theory (MRMP2),[25] incorporating within the active space only the metal-centred orbitals required to describe states within 1 eV of the CASSCF ground state. In all cases, the unoccupied $d_{x^2-y^2}$ orbital was excluded. Similarly, state weighting was restricted to include only states within 1 eV of the CASSCF ground state.

To check for possible mixing between ligand and metal orbitals in the ground and near-to-ground electronic states, additional CASSCF and MRMP2 calculations were performed including the ligand-based HOMO and LUMO orbitals within the active space.

Orbital energies and electronic configurations for the late transition-metal phthalocyanines (MPc, M = Cu, Zn) were obtained from RHF (ZnPc) or ROHF (CuPc) calculations. All molecular orbitals were expanded in the cc-pVDZ atomic orbital basis.[26, 27]

The geometry of ZnPc was optimized at B3LYP/6-31G* and used as a template for other metallophthalocyanines, without any further geometry optimization. This is a reasonable approximation, as previous computational and experimental studies indicate that the phthalocyanine ligand is quite rigid[28, 29, 30, 31, 32]. Distances between the central metal ion (M^{2+}) and closest nitrogen (N) atoms are most sensitive to the identity of the central metal atom, but only differ by up to 0.03 Å across the period from MnPc to ZnPc, according to X-ray diffraction data.[29, 30, 31, 32]

This is similar to the uncertainty inherent in using density functional methods to optimize the geometry. For example, previous estimates of the M^{2+}–N distance in ZnPc vary from 1.955 to 2.012 Å, depending on the functional and basis set chosen.[28] Our value of 1.963 Å is within this range, and close to the experimental value of 1.954 Å.[32].

Previous X-ray diffraction studies,[29, 30, 31, 32] also indicate that all four M^{2+}–N distances are equivalent to each other in all systems investigated here, *i.e.* that all molecular structures have D_{4h} symmetry. Therefore, obtaining an optimized geometry for a closed-shell model system is a sensible strategy to avoid complications associated with spin-symmetry breaking in open-shell systems and those with degenerate ground states, which can lead to artifactual molecular symmetry breaking and substantial errors in calculated state energies.[33, 12] All CASSCF and MRMP2 calculations were run in D_{2h} symmetry, as the largest Abelian subgroup of D_{4h}, and the highest applicable symmetry class implemented in GAMESS.

Full geometric data are provided as Supporting Information.

3. Results and Discussion

3.1. Ligand-field models

CASSCF theory becomes a sophisticated explicit ligand field model when the active space is chosen to include the complete set of metal-centred valence atomic orbitals (d orbitals for transition metals). The electrostatic influence of the ligand on the d orbital energies and associated electronic states is captured directly, by explicitly modelling ligand electrons within the mean field approximation, rather than using an effective Hamiltonian formalism.[34]

Applying this approach to a series of metallophthalocyanines (MPc, M = Mn, Fe, Co, Ni, Cu, Zn) yields the molecular orbital energies and ground state electronic configurations illustrated in Figure 2, noting that this CASSCF procedure is the same as Hartree-Fock theory when all d orbitals are occupied (CuPc, ZnPc).

With the exception of ZnPc, the same ligand field orbital splitting pattern is observed for all metallophthalocyanines investigated here. As expected from canonical crystal field arguments,[35] the $d_{x^2-y^2}$ orbital is highest in energy, due to repulsive electrostatic interactions between the electrons in the metal d orbitals and those of the surrounding ligand.

However, the phthalocyanine ligand is not strictly square planar - it is better described as square planar core contained within a macrocyclic system - and nor is it particularly well described using a simple point charge model. This additional complexity is explicitly accounted for in our CASSCF-derived explicit ligand field model, and results in the d_{xy} orbital becoming the most stable, contrary to conventional expectations based upon crystal field models. This is possibly due to attractive dispersion interactions between metal d electrons and the electrons associated with the outer azamethine nitrogen atoms within the macrocycle.

The remaining orbitals protrude out of the plane of the phthalocyanine ring so are not as sensitive to its shape. Therefore,

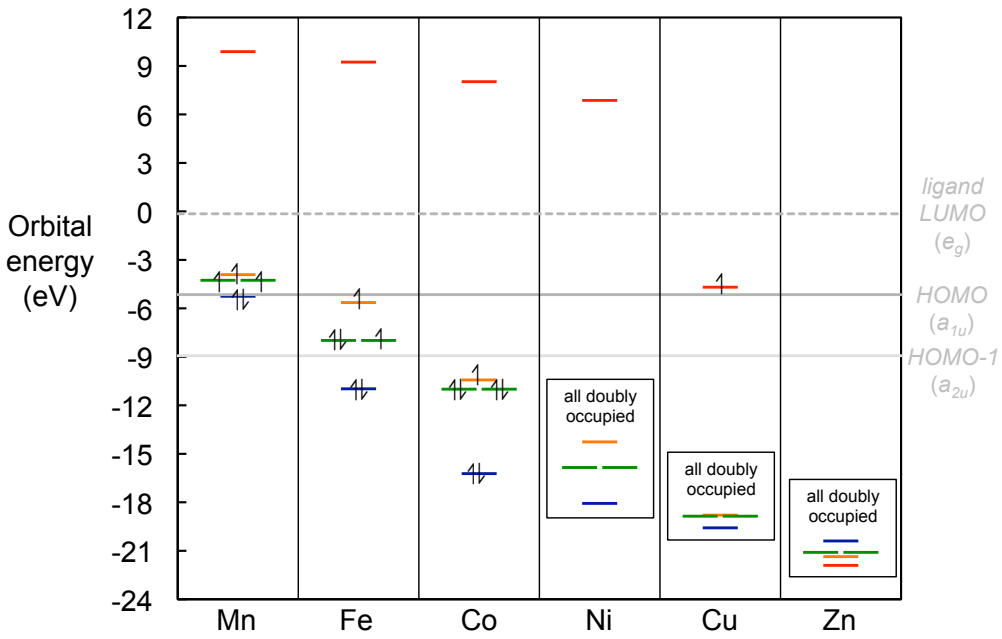

Fig. 2. Ground state electronic configuration of metallophthalocyanines (MPc, M = Mn – Zn) at CASSCF/cc-pVDZ, in an active space comprising a complete set of metal-centred valence orbitals; d_{xy} (blue), d_{xz}/d_{yz} (green), d_{z^2} (orange), $d_{x^2-y^2}$ (red). These orbitals may equivalently be described according to their symmetry labels: b_{2g} (blue), e_g (green), a_{1g} (orange), b_{1g} (red)

they obey the energy orderings predicted by crystal field theory, with the degenerate d_{xz} and d_{yz} orbitals more stable than the d_{z^2} orbital. The overall metal-centred orbital energy ordering is, therefore:

[1] $$d_{xy} < d_{xz}/d_{yz} < d_{z^2} << d_{x^2-y^2}$$

By contrast, canonical square planar crystal field models[35] and some ligand field models[36] predict the d orbital energy ordering:

[2] $$d_{xz}/d_{yz} \approx d_{z^2} < d_{xy} << d_{x^2-y^2}$$

The electronic structure of ZnPc is unusual, with inverted ordering of orbital energies compared to other metallophthalocyanines investigated here. However, all metal-centred orbitals lie at energies significantly lower than the ligand HOMO, and are doubly occupied, so the overall electronic configuration is independent of orbital energy ordering. The Zn nucleus exerts the highest effective nuclear charge on outer valence electrons of all transition metals[35], leading to d orbital energies that are lower and less perturbed by the ligand field. The $3d^{10}4s^0$ electronic configuration at the metal centre corresponds to a dicationic metal ion surrounded by a dianionic ligand, as formally expected.

All metallophthalocyanines investigated here exist as doubly-charged ion-pair complexes with both 4s electrons transferred from the metal atom to the phthalocyanine ligand. The CASSCF-derived ground state electronic configurations illustrated in Figure 2 obey the Aufbau principle, assuming only that distributing electrons amongst low energy (< 0 eV) otherwise unfilled d orbitals is energetically preferable to pairing them within these orbitals.

For NiPc, CuPc and ZnPc, the Aufbau occupations at the metal centre illustrated in Figure 2 and listed in Table 1 are the only plausible ground state electronic configurations, as explained in more detail later. For MnPc, FePc and CoPc, the situation is complicated by the existence of alternative low-energy configurations, generated by rearranging electrons amongst d orbitals. In these cases, the energy of each state, and therefore the identity of the ground state, will depend on a delicate balance between orbital energies and electron pairing energies within orbitals. Further, for CoPc and FePc, partially filled metal orbitals fall below the ligand HOMO, admitting the possibility of ligand-to-metal charge transfer in forming these MPc complexes.

3.2. Other CASSCF models

To further investigate these possibilities, additional CASSCF calculations were performed in active spaces comprising: all occupied metal-centred orbitals (d_{xy},d_{xz},d_{yz},d_{z^2}); and all occupied metal-centred orbitals plus the ligand HOMO and doubly-degenerate LUMO. CASSCF state energies, relative to the CASSCF ground state ($\Delta E_{\mathrm{CASSCF}}$), are presented in Table 1.

Strikingly, the relative energies of low-lying electronic states are similar whether or not ligand orbitals are included in the active space. This means that the ligand HOMO remains doubly occupied and LUMO unoccupied throughout, despite the metal-centred orbitals lying substantially lower in energy than the ligand HOMO. This can only occur if the energetic cost of pairing the electrons within the compact metal d orbitals exceeds the energy associated with *both* placing *and* pairing the electrons within the ligand HOMO.

The other noteworthy observation from Table 1 is the accidental near-degeneracy between the ^3E_g and $^3A_{2g}$ states of

Table 1. Ground and near-to-ground state symmetries, electronic configurations and, where applicable, relative energies at CASSCF/cc-pVDZ and MRMP2/cc-pVDZ, with active spaces comprising the metal-centred orbitals listed in column 3 and, optionally, the ligand HOMO and doubly-degenerate LUMO. Illustrations of ground and near-ground state electronic configurations and their relative energies for MnPc, FePc and CoPc are also provided as Supporting Information.

Metal Atom	State Symmetry	Metal-Centred Orbital Occupancy	$\Delta E_{\mathrm{CASSCF}}$ (eV)	$\Delta E^{\dagger}_{\mathrm{CASSCF}}$ (eV)	$\Delta E_{\mathrm{MRMP2}}$ (eV)	$\Delta E^{\dagger}_{\mathrm{MRMP2}}$ (eV)
Mn	$^4A_{2g}$	$(d_{xy})^2(d_{xz},d_{yz})^{1,1}(d_{z^2})^1$	0	0	0	0
	^4E_g	$(d_{xy})^1(d_{xz},d_{yz})^{2,1}(d_{z^2})^1$	0.506	0.510	0.447	0.354
	$^4B_{1g}$	$(d_{xy})^1(d_{xz},d_{yz})^{1,1}(d_{z^2})^2$	0.555	0.552	0.342	0.344
Fe	$^3A_{2g}$	$(d_{xy})^2(d_{xz},d_{yz})^{1,1}(d_{z^2})^2$	0.027	0.012	0	0
	^3E_g	$(d_{xy})^2(d_{xz},d_{yz})^{2,1}(d_{z^2})^1$	0	0	0.016	0.018
	$^3B_{2g}$	$(d_{xy})^1(d_{xz},d_{yz})^{2,2}(d_{z^2})^1$	0.867	0.880	0.882	0.853
Co	$^2A_{1g}$	$(d_{xy})^2(d_{xz},d_{yz})^{2,2}(d_{z^2})^1$	0	0	0	0
	^2E_g	$(d_{xy})^2(d_{xz},d_{yz})^{2,1}(d_{z^2})^2$	0.609	0.596	0.372	0.344
Ni	$^1A_{1g}$	$(d_{xy})^2(d_{xz},d_{yz})^{2,2}(d_{z^2})^2$	†Ligand-based HOMO ($2a_{1u}$) and doubly-degenerate LUMO ($7e_g$) also included in active space.			
Cu	$^2B_{1g}$	$(d_{xy})^2(d_{xz},d_{yz})^{2,2}(d_{z^2})^2(d_{x^2-y^2})^1$				
Zn	$^1A_{1g}$	$(d_{xy})^2(d_{xz},d_{yz})^{2,2}(d_{z^2})^2(d_{x^2-y^2})^2$				

FePc. In this case, it just so happens that the energy cost associated with transferring an electron to the higher energy d_{z^2} orbital ($^3E_g \rightarrow {}^3A_{2g}$) is almost exactly counterbalanced by an equal energy gain from more facile electron pairing. This counterbalancing effect is also evident in the energies of the near-to-ground ^4E_g and $^4A_{1g}$ CASSCF states of MnPc and the ^2E_g state of CoPc, but not to the same extent.

3.3. Correlated models

Although CASSCF gives a useful qualitative picture of electron behaviour, electron correlation effects must be taken into account to obtain quantitative state energies. MRMP2 relative state energies, $\Delta E_{\mathrm{MRMP2}}$, for MnPc, FePc and CoPc are reported in Table 1, and will be discussed in the context of existing literature results below.

3.4. Ground state assignments

3.4.1. MnPc

Evidence for the ground electronic state of MnPc has previously been gleaned by interpreting spectroscopic data using ligand field theory and/or group theory. A wide range of experiments[11, 12, 37, 38, 9, 39, 30, 40, 41, 42] have been carried out using different sample preparations (argon matrix,[42] thin film,[41, 40, 38, 37, 12] crystalline[39, 43]) and/or spectroscopies (optical absorption,[42, 40, 41] magnetic circular dichroism,[42, 39] photoelectron emission,[12, 37, 38, 41] electron energy loss[40, 38]), leading to conflicting assignments for the ground state of MnPc.

All existing experimental evidence, including magnetic susceptibility measurements,[43, 39] confirm a spin quartet ground state. However, different spatial symmetries have been proposed. Current evidence shows that condensed phase systems with a significant dielectric response but without direct axial interactions (argon matrix,[42] thin films on gold substrate[41, 40, 38, 37, 44, 12]) favour the ^4E_g state over the $^4A_{2g}$ state.

On the other hand, most experimental evidence[45, 46, 47, 48, 43, 49, 50] points to a $^4A_{2g}$ ground state for β-phase crystalline MnPc. Crystal packing leads to axial interactions between manganese centres and the azamethine nitrogen atoms of adjacent molecules, which must, in this case, destabilize the out-of-plane d_{xy}/d_{yz} and d_{z^2} orbitals, and hence favour the $^4A_{2g}$ state.

A recent X-ray absorption and magnetic circular dichroism study of β-MnPc[39] suggests instead a ^4E_g ground state with orbital energy ordering:

$$[3] \qquad d_{xz}/d_{yz} < d_{xy} < d_{z^2} << d_{x^2-y^2}$$

based upon fitting the XMCD spectrum using a ligand-field model, but this is inconsistent with *both* previous experimental[45, 46, 47, 48, 43, 49, 50] *and* previous computational results[12, 51, 52, 53, 54, 55]. However, a reasonable fit can also be found assuming a $^4A_{2g}$ ground state based upon the *ab initio* calculated energy ordering, which is more accurate in some regions of the spectrum, but less in others, relative to the ^4E_g model.

All computational studies,[12, 51, 52, 53, 54, 55] agree on the orbital energy ordering illustrated in Figure 2 and described by equation [1], irrespective of the level of *ab initio* or density functional theory employed. We contend that these metal-centred orbital energies and orderings are more reliable than those obtained from crystal field or parameterized ligand field models, as they explicitly account for electrostatic interactions with the surrounding ligand and are robust with respect to electronic structure model.

Unfortunately, overall state energies are less well modelled, with different density functionals returning different ground state electronic configurations. For example, some studies conclude that the ground state is $^4A_{2g}$[43, 41], with orbital occupancy:

$$(d_{xy})^2(d_{xz},d_{yz})^{1,1}(d_{z^2})^1$$

while others[12, 41, 51] instead arrive at a ^4E_g ground state:

$$(d_{xy})^1(d_{xz}, d_{yz})^{2,1}(d_{z^2})^1$$

To help resolve these differences, high level MRMP2 data are presented in Table 1. These results clearly identify the $^4A_{2g}$ state as the gas-phase ground state, despite more sophisticated accounting for electron correlation somewhat narrowing the energy difference between the ground and excited states. The MRMP2 results are more sensitive to active space composition than their CASSCF counterparts, with inclusion of the doubly degenerate ligand-based e_g LUMO significantly stabilizing the ^4E_g state. These results are broadly consistent with experimental observations that, under different conditions, MnPc assumes either a $^4A_{2g}$ or ^4E_g ground state, but not $^4B_{1g}$.

However, it also seems clear that a combination of yet more sophisticated electron correlation models and inclusion of environmental effects are required to explain the observed ^4E_g ground state for α-crystalline and thin film MnPc. Within the *ab initio* explicit ligand field model alone, significant additional stabilization of the d_{xy}/d_{yz} orbitals in the condensed phase would be required to tip the balance in favour of the ^4E_g state, although configurational mixing within correlated models also contributes to stabilizing the ^4E_g state relative to $^4A_{2g}$, as noted above.

The electronic ground state of β-MnPc is easier to assign on the basis of our results, also taking into account existing experimental evidence,[45, 46, 47, 48, 43, 49, 50] particularly magnetic susceptibility measurements[16]. We conclude that it is best described as a $^4A_{2g}$ ground state, which may mix with a low-lying ^4E_g excited state through spin-orbit coupling. This is the only assignment that is consistent with all existing experimental data and high level computational results.

3.4.2. FePc

There is consensus within the experimental and computational literature[16, 56, 57, 58, 36, 18, 28, 59, 61, 62, 41] that it is difficult to assign a unique ground state for FePc, due to the presence of two near-degenerate triplet states, one of which is an orbitally degenerate ^3E_g state and the other which is orbitally non-degenerate.

Disagreement arises as to which orbitally non-degenerate state lies near the ^3E_g state, with different assumed orbital energy orderings producing different predictions. In particular, a number of experimental studies use ligand field theory to interpret the observed spectra, assuming canonical square planar crystal field energy orderings.[16, 56, 57, 58, 36] These studies uniformly predict a low-lying $^3B_{2g}$ state with orbital occupancy

$$(d_{z^2})^1(d_{xz}, d_{yz})^{2,2}(d_{xy})^1$$

that is near-degenerate with a ^3E_g state:

$$(d_{z^2})^2(d_{xz}, d_{yz})^{2,1}(d_{xy})^1$$

However, our computational results (Table 1) instead reveal a low-lying $^3A_{2g}$ state:

$$(d_{xy})^2(d_{xz}, d_{yz})^{1,1}(d_{z^2})^2$$

that is near-degenerate with a *different* ^3E_g state:

$$(d_{xy})^2(d_{xz}, d_{yz})^{2,1}(d_{z^2})^1$$

Both of these states are significantly more stable than the alternative ^3E_g and $^3B_{2g}$ states preferred by the parameterized ligand field model, with the $^3B_{2g}$ state the lower in energy of the two.

As discussed above in the case of MnPc, we contend that explicit ligand field models provide a more accurate representation of ligand field effects and orbital energies than implicit ligand field models. For FePc, the case in favour of *ab initio* electronic structure modelling is particularly strong, with: internal consistency in orbital ordering across the period (Figure 2); consistency with other computational results [18, 28, 59]; consistency with experimental results including magnetic circular dichroism[60], Mössbauer [61], X-ray absorption[62, 41] and X-ray magnetic circular dichroism[62, 41] spectra.

For example, a recent experimental study of thin film samples on a gold substrate by Kroll *et al.*[41] concludes that X-ray absorption and photoemission spectra are most compatible with a ^3E_g ground state, although the possibility of a $^3A_{2g}$ ground state cannot be entirely excluded. Similarly, Mössbauer spectroscopy[61] and magnetic susceptibility[20] measurements on crystalline α-FePc firmly establish a ^3E_g ground state, with occupied orbitals:

$$(d_{xy})^2(d_{xz}, d_{yz})^{2,1}(d_{z^2})^1$$

Again, this is consistent with our computational results, but not with parameterized ligand field model interpretations. Additionally, it is likely that environmental effects have broken the near-degeneracy between the ^3E_g and $^3A_{2g}$ states in this strongly interacting condensed-phase system, preferentially stabilizing the ^3E_g state.

However, environmental effects cannot rationalize differences between previous experimentally and computationally inferred ground-state assignments, because the energy differences between the low-lying ^3E_g and $^3A_{2g}$ states and the $^3B_{2g}$ excited state are too large. Therefore, disagreements as to the nature of the low-lying orbitally non-degenerate state must be due to the underlying model used to interpret the experimental observations.

Recent magnetic susceptibility, X-ray absorption and X-ray magnetic circular dichroism measurements on thin film samples suggest that a complete picture of the electronic structure of FePc can be obtained only if spin-orbit coupling between low-lying near-degenerate electronic states is taken into account.[58, 36] However, these studies invoke ligand field models that assume canonical square planar orbital ordering, and so predict a low-lying $^3B_{2g}$ state, which is hard to justify against the weight of computational evidence presented both here and in the literature.[61, 62, 18, 28, 59, 41].

We anticipate that a full and final model of the electronic structure of FePc in the gas phase and/or weakly interacting condensed phases will be arrived at once spin-orbit coupling between the computationally identified ^3E_g and $^3A_{2g}$ states is taken into account.[34] These states may be considered degenerate to within the intrinsic accuracy of the electronic structure models applied here.

3.4.3. CoPc

For CoPc, the d_{xy} orbital is much lower in energy than the d_{xz}/d_{yz} and d_{z^2} orbitals (Figure 2) and so only two ground state electronic configurations are possible; an orbitally degenerate ^2E_g state and an orbitally non-degenerate $^2A_{1g}$ state, with the electronic configurations listed in column 3 of Table 1.

Experimental studies clearly identify the $^2A_{1g}$ state as the ground state, irrespective of sample preparation.[41, 63] This is supported by our MRMP2 results (Table 1) and some[55] but not all[28] previous DFT studies.

3.4.4. NiPc, CuPc, ZnPc

The electronic ground states of NiPc and ZnPc may be clearly and unambiguously assigned as spin-singlet states of A_{1g} symmetry, based upon the CASSCF orbital energies and occupancies illustrated in Figure 2. These uncontentious assignments are unanimously supported in the literature.[18, 53, 28, 64, 65, 66, 67, 68, 69, 70, 71, 72, 73, 74, 75, 76, 18]

For CuPc, inspection of Figure 2 suggests that an alternative configuration may be possible, with two electrons in the d_{z^2} orbital and only one in the ligand HOMO, which would correspond to a closed-shell metal cation surrounded by a radical anion ligand. However, this physically implausible state is higher in energy than the depicted configuration, *both* because the $d_{x^2-y^2}$ orbital is less stable than the ligand HOMO *and* because it is harder to pair electrons within the more compact metal-centred orbital. This analysis is supported by previous experimental[77, 78, 79, 80, 81] and computational[82, 77, 78, 83, 18, 79, 84] studies that agree on the ground state configuration shown in Figure 2.

The ground state assignments for NiPc, CuPc and ZnPc summarized in Table 1 are also consistent with experimental observations. Magnetic circular dichroism[85] and optical absorption[86] spectra of these systems are practically identical, containing only ligand-based transitions that occur without any change in electronic configuration at the metal centre.

4. Conclusions

Discrepancies between ground state assignments of metallophthalocyanines - particularly MnPc and FePc - result largely from different models being used to analyse experimental data. However, only *ab initio* (CASSCF) derived explicit ligand field models provide consistent and coherent orbital energies *and* state assignments for all MPcs investigated here. Correlated models provide more accurate state energies, but do not significantly alter the qualitative picture provided by multireference mean-field models. Some discrepancies between experimental and computational ground state assignments remain even at MRMP2, but these are small and can be attributed to environmental effects and incomplete modelling of electron correlation. Our computational results align exactly with the recent experimental X-ray spectroscopy measurements of Kroll *et al*, demonstrating the power of synergy between theory and experiment in establishing the electronic structure of molecules and materials.

5. Acknowledgement

The authors acknowledge the contribution of NeSI high-performance computing facilities to the results of this research. New Zealand's national facilities are provided by the NZ eScience Infrastructure and funded jointly by NeSI's collaborator institutions and through the Ministry of Business, Innovation & Employment's Research Infrastructure programme. This work was also supported by the Marsden Fund Council from Government funding, administered by the Royal Society of New Zealand.

References

1. Milgram, L. R. *The Colours of Life. An Introduction to the Chemistry of Porphyrins and Related Compounds.*; Oxford University Press: Oxford, 1997.
2. Löbbert, G. *Phthalocyanines*; Wiley-VCH Verlag GmbH & Co. KGaA, 2000.
3. Bonnett, R. *Chem. Soc. Rev.* **1995**, *24*, 19–33.
4. Ghosh, A.; Vangberg, T.; Gonzalez, E.; Taylor, P. *J. Porph. Phthal.* **2001**, *5*, 345–356.
5. Banfi, S.; Caruso, E.; Buccafurni, L.; Ravizza, R.; Gariboldi, M.; Monti, E. *J. Organomet. Chem.* **2007**, *692*, 1269–1276.
6. Moreira, L. M.; dos Santos, F. V.; Lyon, J. P.; Maftoum-Costa, M.; Pacheco-Soares, C.; da Silva, N. S. *Aust. J. Chem.* **2008**, *61*, 741–754.
7. Ogbodu, R. O.; Nyokong, T. *Spectrochim. Acta A* **2015**, *151*, 174–183.
8. Saini, S. K.; Jena, A.; Dey, J.; Sharma, A. K.; Singh, R. *Mag. Res. Imaging* **1995**, *13*, 985–990.
9. Johnson, P. S.; Garcia-Lastra, J. M.; Kennedy, C. K.; Jersett, N. J.; Boukahil, I.; Himpsel, F. J.; Cook, P. L. *J. Chem. Phys.* **2014**, *140*, 114706.
10. Mack, J.; Stillman, M. J. *The Porphyrin Handbook*; Elsevier Science, 2003; Vol. 16, Chapter 103, pp 44–116.
11. Bidermane, I.; Brumboiu, I. E.; Totani, R.; Grazioli, C.; Shariati-Nilsson, M. N.; Herper, H. C.; Eriksson, O.; Sanyal, B.; Ressel, B.; de Simone, M.; Lozzi, L.; Brena, B.; Puglia, C. *J. Elec. Spec.* **2015**, *205*, 92–97.
12. Brumboiu, I. E.; Totani, R.; de Simone, M.; Coreno, M.; Grazioli, C.; Lozzi, L.; Herper, H. C.; Sanyal, B.; Erikssont, O.; Puglia, C.; Brena, B. *J. Phys. Chem. A* **2014**, *118*, 927–932.
13. Calzolari, A.; Ferretti, A.; Nardelli, M. B. *Nanotech.* **2007**, *18*, 424013.
14. Ahlund, J.; Nilson, K.; Schiessling, J.; Kjeldgaard, L.; Berner, S.; Martensson, N.; Puglia, C.; Brena, B.; Nyberg, M.; Luo, Y. *J. Chem. Phys.* **2006**, *125*, 034709.
15. Arillo-Flores, O. I.; Fadlallah, M. M.; Schuster, C.; Eckern, U.; Romero, A. H. *Phys. Rev. B* **2013**, *87*, 165115.
16. Barraclough, C. G.; Martin, R. L.; Mitra, S.; Sherwood, R. C. *J. Chem. Phys.* **1970**, *53*, 1643–1648.
17. Brena, B.; Puglia, C.; de Simone, M.; Coreno, M.; Tarafder, K.; Feyer, V.; Banerjee, R.; Gothelid, E.; Sanyal, B.; Oppeneer, P. M.; Eriksson, O. *J. Chem. Phys.* **2011**, *134*, 074312.
18. Bruder, I.; Schoeneboom, J.; Dinnebier, R.; Ojala, A.; Schaefer, S.; Sens, R.; Erk, P.; Weis, J. *Org. Elec.* **2010**, *11*, 377–387.
19. Coppens, P.; Li, L.; Zhu, N. J. *J. Am. Chem. Soc.* **1983**, *105*, 6173–6174.

20. Dale, B. W.; Williams, R. J. P.; Johnson, C. E.; Thorp, T. L. *J. Chem. Phys.* **1968**, *49*, 3441–3444.
21. Atanasov, M.; Ganyushin, D.; Sivalingam, K.; Neese, F. *Struct. Bond.* **2012**, *143*, 149–220.
22. Ballhausen, C. J. *Ligand field theory*; McGraw-Hill, New York, 1962.
23. Schmidt, M. W.; Gordon, M. S. *Ann. Rev. Phys. Chem.* **1998**, *49*, 233–266.
24. Schmidt, M. W.; Baldridge, K. K.; Boatz, J. A.; Elbert, S. T.; Gordon, M. S.; Jensen, J. H.; Koseki, S.; Matsunaga, N.; Nguyen, K. A.; Su, S. J.; Windus, T. L.; Dupuis, M.; Montgomery, J. A. *J. Comp. Chem.* **1993**, *14*, 1347–1363.
25. Hirao, K. *Chem. Phys. Lett.* **1992**, *190*, 374–380.
26. Kendall, R. A.; Dunning Jr, T. H.; Harrison, R. J. *J. Chem. Phys* **1992**, *96*, 6796–6806.
27. Woon, D. E.; Dunning Jr, T. H. *J. Chem. Phys.* **1993**, *98*, 1358–1371.
28. Liao, M. S.; Scheiner, S. *J. Chem. Phys.* **2001**, *114*, 9780–9791.
29. Mason, R.; Williams, G. A.; Fielding, P. E. *J. Chem. Soc., Dalton Trans.* **1979**, 676–683.
30. Kirner, J. F.; Dow, W.; Scheidt, W. R. *Inorg. Chem.* **1976**, *15*, 1685–1690.
31. Brown, C. J. *Journal Chem. Soc. A* **1968**, 2488–2493.
32. Ruan, C. Y.; Mastryukov, V.; Fink, M. *J. Chem. Phys.* **1999**, *111*, 3035–3041.
33. Davidson, E. R.; Borden, W. T. *J. Phys. Chem.* **1983**, *87*, 4783–4790.
34. Sundararajan, M.; Ganyushin, D.; Ye, S.; Neese, F. *Dalton Trans.* **2009**, 6021–6036.
35. Shriver, D. F.; Atkins, P. W. *Shriver and Atkins' Inorganic Chemistry*; Oxford University Press, USA, 1999.
36. Fernandez-Rodriguez, J.; Toby, B.; van Veenendaal, M. *Phys. Rev. B* **2015**, *91*, 214427.
37. Grobosch, M.; Mahns, B.; Loose, C.; Friedrich, R.; Schmidt, C.; Kortus, J.; Knupfer, M. *Chem. Phys. Lett.* **2011**, *505*, 122–125.
38. Grobosch, M.; Schmidt, C.; Kraus, R.; Knupfer, M. *Org. Elec.* **2010**, *11*, 1483–1488.
39. Kataoka, T.; Sakamoto, Y.; Yamazaki, Y.; Singh, V. R.; Fujimori, A.; Takeda, Y.; Ohkochi, T.; Fujimori, S.; Okane, T.; Saitoh, Y.; Yamagami, H.; Tanaka, A. *Solid State Comm.* **2012**, *152*, 806–809.
40. Kraus, R.; Grobosch, M.; Knupfer, M. *Chem. Phys. Lett.* **2009**, *469*, 121–124.
41. Kroll, T.; Kraus, R.; Schoenfelder, R.; Aristov, V. Y.; Molodtsova, O. V.; Hoffmann, P.; Knupfer, M. *J. Chem. Phys.* **2012**, *137*, 054306.
42. Williamson, B. E.; VanCott, T. C.; Boyle, M. E.; Misener, G. C.; Stillman, M. J.; Schatz, P. N. *J. Am. Chem. Soc.* **1992**, *114*, 2412–2419.
43. Mitra, S.; Gregson, A. K.; Hatfield, W. E.; Weller, R. R. *Inorg. Chem.* **1983**, *22*, 1729–1732.
44. Petraki, F.; Peisert, H.; Hoffmann, P.; Uihlein, J.; Knupfer, M.; Chassé, T. *J. Phys. Chem.* **2012**, *116*, 5121–5127.
45. Turner, P.; Gunter, M. J. *Inorg. Chem.* **1994**, *33*, 1406–1415.
46. Barraclough, C. G.; Martin, R. L.; Mitra, S.; Sherwood, R. C. *J. Chem. Phys.* **1970**, *53*, 1638–1642.
47. Barraclough, C. G.; Gregson, A.; Mitra, S. *J. Chem. Phys.* **1974**, *60*, 962–968.
48. Miyoshi, H. *Bull. Chem. Soc. Japan* **1974**, *47*, 561–565.
49. Labarta, A.; Molins, E.; Tejada, J. *Z. Phys. B* **1985**, *58*, 299–304.
50. Lever, A. B. P. *J. Chem. Soc.* **1965**, *336*, 1821–1829.
51. Liao, M. S.; Watts, J. D.; Huang, M. J. *Inorg. Chem.* **2005**, *44*, 1941–1949.
52. Wu, W.; Kerridge, A.; Harker, A. H.; Fisher, A. J. *Phys. Rev. B* **2008**, *77*, 184403.
53. Garcia-Lastra, J. M.; Cook, P. L.; Himpsel, F. J.; Rubio, A. *J. Chem. Phys.* **2010**, *133*, 151103.
54. Marom, N.; Kronik, L. *App. Phys. A - Mat. Sci. & Proc.* **2009**, *95*, 165–172.
55. Reynolds, P. A.; Figgis, B. N. *Inorg. Chem.* **1991**, *30*, 2294–2300.
56. Miedema, P. S.; Stepanow, S.; Gambardella, P.; de Groot, F. M. F. *J. Phys: Conf. Series* **2009**, *190*, 012143.
57. Stepanow, S.; Miedema, P. S.; Mugarza, A.; Ceballos, G.; Moras, P.; Cezar, J. C.; Carbone, C.; de Groot, F. M. F.; Gambardella, P. *Phys. Rev. B* **2011**, *83*, 220401.
58. Kuz'min, M. D.; Savoyant, A.; Hayn, R. *J. Chem. Phys.* **2013**, *138*, 244308.
59. Liao, M. S.; Scheiner, S. *J. Chem. Phys.* **2002**, *116*, 3635–3645.
60. Stillman, M. J.; Thomson, A. J. *J. Chem. Soc. Faraday Trans. II* **1974**, *70*, 790–804.
61. Filoti, G.; Kuz'min, M. D.; Bartolome, J. *Phys. Rev. B* **2006**, *74*, 134420.
62. Kuz'min, M. D.; Hayn, R.; Oison, V. *Phys. Rev. B* **2009**, *79*, 024413.
63. Janczak, J.; Kubiak, R. *Inorg. Chim. Acta* **2003**, *342*, 64–76.
64. VanCott, T. C.; Rose, J. L.; Misener, G. C.; Williamson, B. E.; Schrimpf, A. E.; Boyle, M. E.; Schatz, P. N. *J. Phys. Chem.* **1989**, *93*, 2999–3011.
65. Ueno, L. T.; Jayme, C. C.; Silva, L. R.; Pereira, E. B.; de Oliveira, S. M.; Machado, A. E. H. *J. Braz. Chem. Soc.* **2012**, *23*, 2237–2247.
66. Theisen, R. F.; Huang, L.; Fleetham, T.; Adams, J. B.; Li, J. *J. Chem. Phys.* **2015**, *142*, 094310.
67. Ricciardi, G.; Rosa, A.; Baerends, E. J. *J. Phys. Chem. A* **2001**, *105*, 5242–5254.
68. Plows, F. L.; Jones, A. C. *J. Mol. Spec.* **1999**, *194*, 163–170.
69. Peralta, G. A.; Seth, M.; Zhekova, H.; Ziegler, T. *Inorg. Chem.* **2008**, *47*, 4185–4198.
70. Peralta, G. A.; Seth, M.; Ziegler, T. *Inorg. Chem.* **2007**, *46*, 9111–9125.
71. Nguyen, K. A.; Pachter, R. *J. Chem. Phys.* **2001**, *114*, 10757–10767.
72. Nemykin, V. N.; Hadt, R. G.; Belosludov, R. V.; Mizuseki, H.; Kawazoe, Y. *J. Phys. Chem. A* **2007**, *111*, 12901–12913.
73. Mack, J.; Stillman, M. J. *J. Phys. Chem.* **1995**, *99*, 7935–7945.
74. Krasnikov, S. A.; Preobrajenski, A. B.; Sergeeva, N. N.; Brzhezinskaya, M. M.; Nesterov, M. A.; Cafolla, A. A.; Senge, M. O.; Vinogradov, A. S. *Chem. Phys.* **2007**, *332*, 318–324.
75. Guo, M.; He, R.; Dai, Y.; Shen, W.; Li, M.; Zhu, C.; Lin, S. H. *J. Chem. Phys.* **2012**, *136*, 144313.
76. Gantchev, T.; van Lier, J.; Hunting, D. *Rad. Phys. Chem.* **2005**, *72*, 367–379.
77. Downes, J. E.; McGuinness, C.; Glans, P. A.; Learmonth, T.; Fu, D. F.; Sheridan, P.; Smith, K. E. *Chem. Phys. Lett.* **2004**, *390*, 203–207.
78. Evangelista, F.; Carravetta, V.; Stefani, G.; Jansik, B.; Alagia, M.; Stranges, S.; Ruocco, A. *J. Chem. Phys.* **2007**, *126*, 124709.
79. Cook, P. L.; Yang, W.; Liu, X.; Maria Garcia-Lastra, J.; Rubio, A.; Himpsel, F. J. *J. Chem. Phys.* **2011**, *134*, 204707.

80. Schwieger, T.; Peisert, H.; Golden, M. S.; Knupfer, M.; Fink, J. *Phys. Rev. B* **2002**, *66*, 155207.
81. Dunford, C. L.; Williamson, B. E. *The Journal of Physical Chemistry A* **1997**, *101*, 2050–2054.
82. Henriksson, A.; Sundbom, M.; Roos, B. *Theor. Chim. Acta* **1972**, *27*, 303–313.
83. Marom, N.; Hod, O.; Scuseria, G. E.; Kronik, L. *J. Chem. Phys.* **2008**, *128*, 164107.
84. Marom, N.; Ren, X.; Moussa, J. E.; Chelikowsky, J. R.; Kronik, L. *Phys. Rev. B* **2011**, *84*, 195143.
85. Mack, J.; Stillman, M. J.; Kobayashi, N. *Coord. Chem. Rev.* **2007**, *251*, 429–453.
86. Wolberg, A.; Manassen, J. *J. Am. Chem. Soc.* **1970**, *92*, 2982–2991.